Nuclear Instruments and Methods in Physics Research A 766 (2014) 101–106

Contents lists available at ScienceDirect

Nuclear Instruments and Methods in Physics Research A

journal homepage: www.elsevier.com/locate/nima

The CBM RICH project

J. Adamczewski-Musch [a], K.-H. Becker [b], S. Belogurov [c], N. Boldyreva [d], A. Chernogorov [c], C. Deveaux [e], V. Dobyrn [d], M. Dürr [e], J. Eom [f], J. Eschke [a], C. Höhne [e], K.-H. Kampert [b], V. Kleipa [a], L. Kochenda [d], B. Kolb [a], J. Kopfer [b], P. Kravtsov [d], S. Lebedev [e], E. Lebedeva [e], E. Leonova [d], S. Linev [a], T. Mahmoud [e], J. Michel [a], N. Miftakhov [d], Y. Nam [f], W. Niebur [a], K. Oh [f], E. Ovcharenko [c], C. Pauly [b,*], J. Pouryamout [b], S. Querchfeld [b], J. Rautenberg [b], S. Reinecke [b], Y. Riabov [d], E. Roshchin [d], V. Samsonov [d], J. Song [f], O. Tarasenkova [d], T. Torres de Heidenreich [a], M. Traxler [a], C. Ugur [a], E. Vznuzdaev [d], M. Vznuzdaev [d], J. Yi [f], I.-K. Yoo [f]

[a] GSI Darmstadt, Germany
[b] University Wuppertal, Germany
[c] ITEP Moscow, Russia
[d] PNPI Gatchina, Russia
[e] University Gießen, Germany
[f] Pusan National University, Republic of Korea

ARTICLE INFO

Available online 11 June 2014

Keywords:
RICH
CBM
Cherenkov radiation

ABSTRACT

The Compressed Baryonic Matter (CBM) experiment will study the properties of super dense nuclear matter by means of heavy ion collisions at the future FAIR facility. An integral detector component is a large Ring Imaging Cherenkov detector with CO_2 gas radiator, which will mainly serve for electron identification and pion suppression necessary to access rare dileptonic probes like e^+e^- decays of light vector mesons or J/Ψ. We describe the design of this future RICH detector and focus on results obtained by building a CBM RICH detector prototype tested at CERN-PS.

1. Introduction

Studying the phase diagram of strongly interacting matter in the region of highest net-Baryon density and moderate temperature is the driving motivation behind the Compressed Baryonic Matter experiment [1], CBM, being built at the future FAIR facility in Darmstadt, Germany. Using fixed target heavy ion collisions with beam energies up to 35 AGeV (Au+Au) at unprecedented interaction rates up to 10 MHz will allow one to investigate many different facets of QCD at high density by using different probes. Key topics of the CBM physics program are the search for a first-order phase transition, and the experimental verification of a critical endpoint. The spontaneous breaking of the Chiral Symmetry in QCD, which is responsible for a large part of the masses of hadrons, is expected to be (partially) restored beyond this phase transition. This will affect the mass spectral shape of the light vector mesons, such as the ρ meson, which has a life time short enough ($\tau \approx 10^{-24}$ s) to decay while still being embedded in the dense medium of the early collision fireball. Rare dileptonic decays of the ρ meson (BR $\approx 10^{-4}$) allow one to reconstruct the spectral function via l^+l^- invariant mass, with the leptons being undisturbed by further strong interactions. Excellent particle identification, in particular e/π separation, is a key requirement for separating these rare probes from the overwhelming background of up to 1000 charged pion/kaon tracks in a typical central Au+Au collision at 35 AGeV. Within the CBM detector setup, the CBM RICH detector serves as the main identification tool for electrons up to ≈8 GeV/c.

2. The CBM RICH detector

In Fig. 1 a sketch of the CBM experimental setup in electron configuration is shown. The RICH is designed as a classical focusing RICH detector, using CO_2 gas at 2 mbar overpressure as a radiator ($\gamma_{th} = 33, p_{th,\pi} = 4.65$ GeV/c). The choice of radiator gas is motivated (beside its refractive index) by good availability and easy handling (in contrast e.g. to CF_4), and low scintillation light yield.

* Corresponding author.
E-mail address: pauly@physik.uni-wuppertal.de (C. Pauly).

http://dx.doi.org/10.1016/j.nima.2014.05.071
0168-9002/

The latter is important in view of the high rate of charged tracks passing the RICH detector (Fig. 2).

Focusing of induced Cherenkov light is achieved by a large, multi-segmented spherical mirror system of 13 m^2 (two half mirrors above/below beampipe) with curvature radius 3 m. Glass mirror tiles (40×40cm, 6 mm thick) with Al+MgF_2 reflective coating (reflectivity 85% over large wavelength range) will be used, mounted to a light-weight aluminum frame (see [2] for further details).

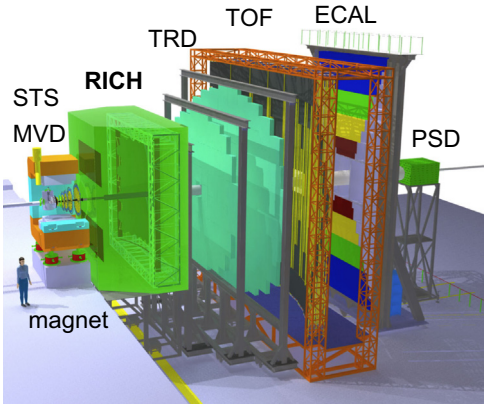

Fig. 1. Layout of the CBM detector setup in electron configuration.

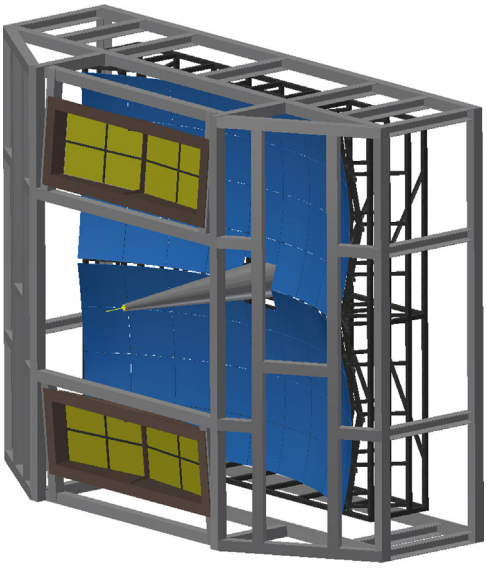

Fig. 2. Sketch of the CBM RICH detector.

The photon detection system covers a total active area of 2.4 m^2. Either Multianode Photomultipliers (MAPMTs) or Microchannel Plate Detectors (MCP-PMTs) with UV-transparent window will be used, matching well the transmission range of CO_2 (transmission cut-off at 180 nm). The use of a wavelength shifting coating applied on the PMT window is considered in order to further increase the UV efficiency (see [3] for details). The readout pixel size is 6×6 mm^2, leading to a total of 55k readout channels. The usage of Photomultipliers will require additional iron shielding boxes around the photon detectors in order to reduce the magnetic stray field of the close-by dipole magnet to values ≤ 1–2 mT at the photo cathode.

The proposed design of the CBM RICH detector has been summarized in a comprehensive Technical Design Report [4], further details can be also found in Ref. [5].

3. The CBM RICH prototype

A full scale prototype detector has been built in order to validate the detector design, to cross check the performance simulations, and to test the interplay of all the components. A sketch and a photo of this prototype can be seen in Fig. 3. It resembles the final RICH in all important dimensions, in particular the radiator length (1.7 m) and the curvature radius of the mirror (3 m), as well as in the choice of radiator gas CO_2. It already uses many components as foreseen for the final RICH, like the mirror tiles and the gas purification and control system. This prototype was tested during two test beam campaigns at CERN-PS in 2011 and 2012, using a mixed electron–pion beam of selectable momenta up to 10 GeV/c. Two additional threshold Cherenkov counters in the beam line allowed for independent particle identification, allowing to study the particle ID performance of the prototype.

The prototype photon detector, shown in Fig. 4, combined several different sensor candidates in a single detection plane. In 2012, it was based on 10 pc Hamamatsu H8500 type MAPMTs (UV-glass, Bialkali cathode, design baseline), 2 Hamamatsu H10966 (8-stage version of H8500, UV-glass, Superbialkali cathode), 8 Hamamatsu R11265 (1 inch, similar pixel size as H8500, SBA-cathode), and 3 Photonis XP85012 MCPs (quartz window and BA cathode). The signal readout was based on the nXYTer ASIC [6], providing fully self-triggered readout.

The focusing mirror, consisting of 4 mirror tiles 40×40 cm^2 each, was mounted on a special gimbal frame providing remote controlled tilting of the mirror around *X*- and *Y*-axis during data taking. This allowed one to move the Cherenkov ring on different regions of the camera in order to directly compare the performance of the different sensor candidates under identical conditions. A typical integrated electron ring image is shown as overlay

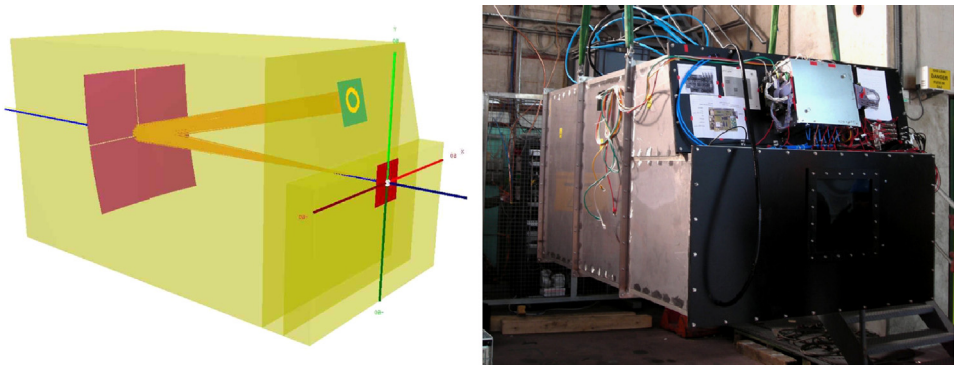

Fig. 3. Sketch and photograph of the CBM RICH prototype used during two test beams at CERN-PS in 2011 and 2012.

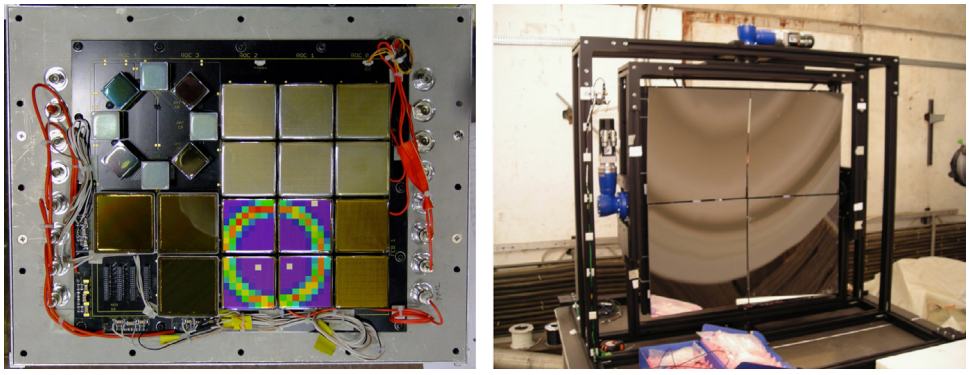

Fig. 4. The photon detection plane with various different sensor devices as instrumented in 2012 CERN beam test (left). The prototype mirror frame (right).

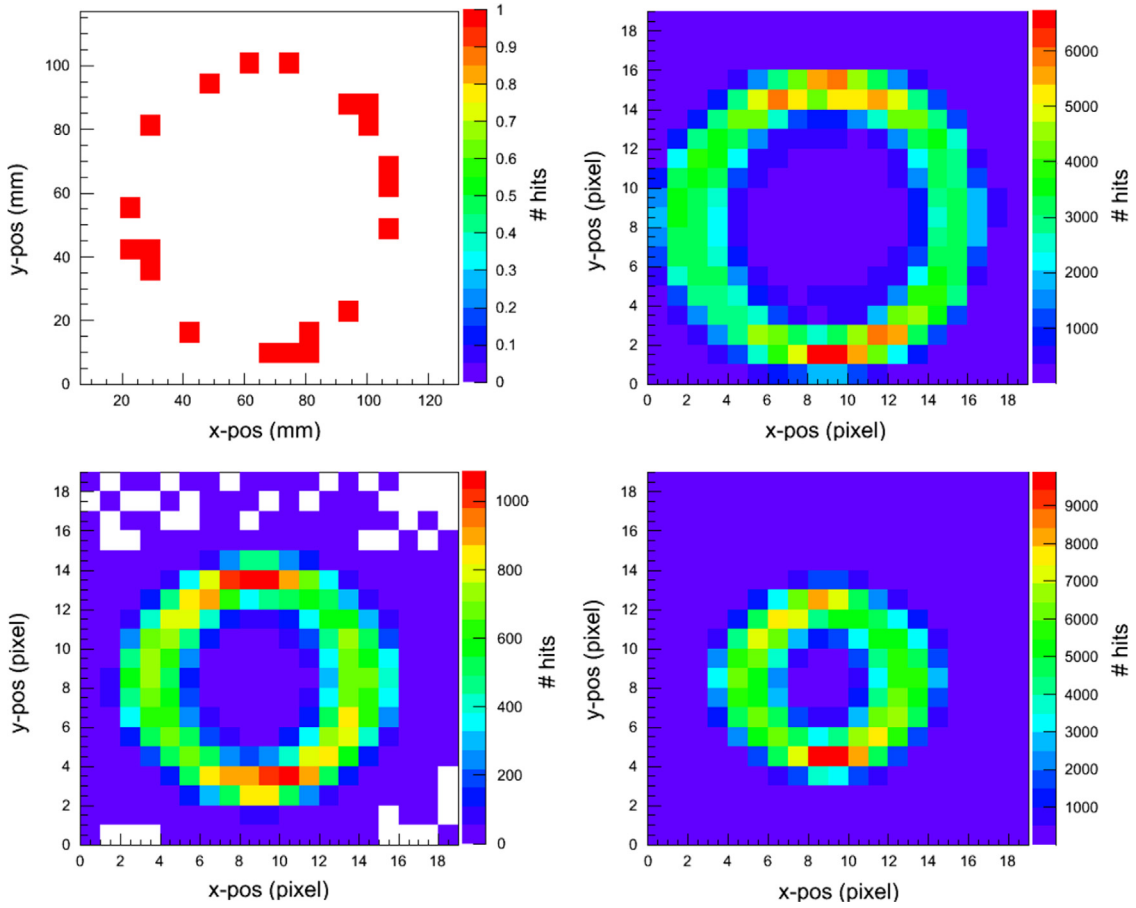

Fig. 5. Typical single electron event (upper left) and integrated ring images for particles identified as electrons (upper right), muons (lower left) and pions (lower right) at 5 GeV/c beam momentum.

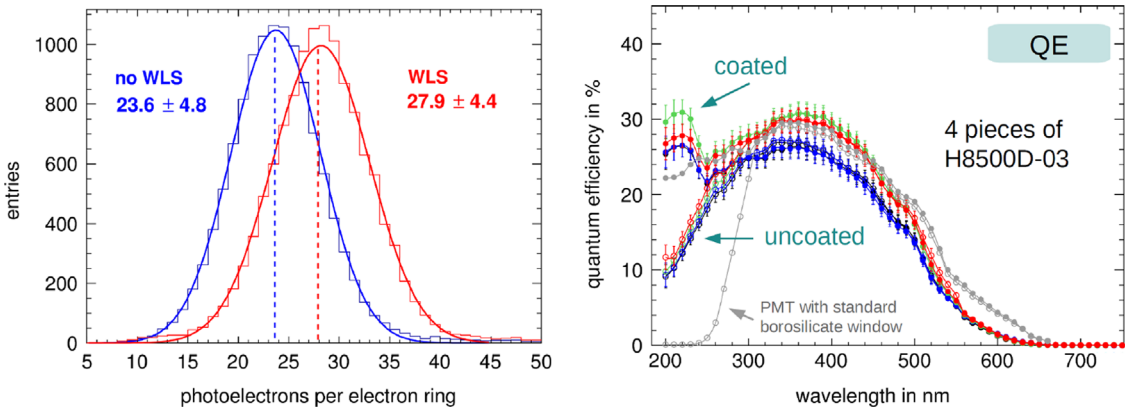

Fig. 6. Multiplicity distribution of detected photons per electron ring measured for H8500 MAPMTs with and without WLS coating (left). The WLS coating increases the quantum efficiency at short wave length (below 300 nm) (right).

in Fig. 4. Some of the sensors were initially coated with wavelength shifting coating (light grey sensor surface in Fig. 4); this coating was later removed during the beam time in order to allow for a precise quantitative evaluation of the WLS.

The prototype gas system included a gas purification loop with a purifier and a dryer for removal of oxygen and moisture, which were reduced in routine operation down to levels of 100 ppm and 200 ppm respectively. No significant effect on the photon hit multiplicity could be observed even after artificial contamination up to 1% oxygen and 1100 ppm moisture.

3.1. Results on photon multiplicity and ring reconstruction

Crucial for the performance of any RICH detector is the number of detected photons per Cherenkov ring, as well as shape and resolution of the obtained ring image, since they directly affect the efficiency of ring finding and radius determination. This is even more true in case of the CBM RICH in view of the large expected ring density (up to 100 rings per central Au+Au collision due to large number of pions and secondary conversion electrons). Fig. 5 shows a typical single event ring image of an electron ring (upper left) and integrated ring images of (externally) selected electrons, muons and pions obtained at 5 GeV/c beam momentum. The width of the integrated ring images is mainly determined by the angular divergence of the beam, and not by the single ring resolution. The number of detected hits per electron ring is shown in Fig. 6, it follows nicely a Gaussian shape. Without additional WLS-coating, around 23–24 hits/e^--ring are detected with H8500 MAPMTs, depending on the type of photo sensor/ring position on the camera. Using a WLS coating on the glass window of the MAPMT increases the photon yield by $\approx$18%. These hit multiplicity numbers include $\approx$10% additional hits due to cross talk to neighboring channels, which could also be extracted from the data. The photon yield is in a very good agreement with results from a full GEANT3 based Monte Carlo simulation of the prototype, taking into account the measured spectral shape of the quantum efficiency of individual sensors, and assuming a realistic collection efficiency of the MAPMTs in the order of 85%.

Fig. 6 (right) shows some of the measured quantum efficiency curves for H8500 PMTs before and after removal of the WLS coating. The WLS coating increases the quantum efficiency significantly below 250 nm basically without any decrease in the visible range thanks to a careful optimization of the WLS layer thickness.

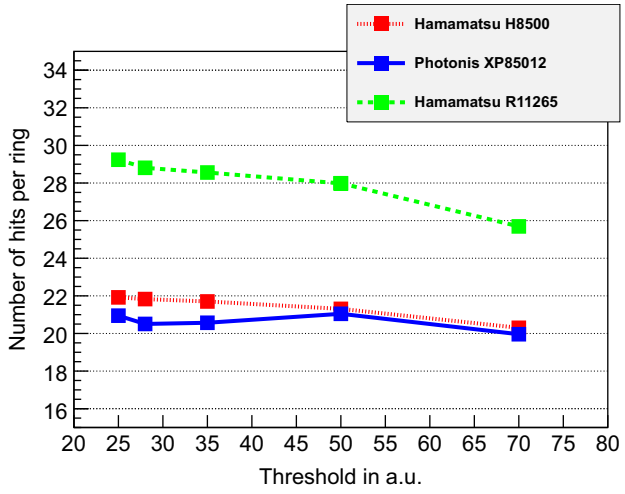

Fig. 7. Comparison of detected hits per electron Cherenkov ring (after subtracting cross talk hits) for Hamamatsu R11265 (SBA+UV-window), H8500 (BA+UV-window), and Photonis XP85012 MCP (BA+quartz).

3.2. Comparison of different sensors

A comparison of the number of detected photons per electron Cherenkov ring for three different sensor candidates is shown in Fig. 7 as a function of detection threshold (in arbitrary units). The number of detected hits shown here is corrected for additional cross talk hits, and also for different spatial coverage of the ring image for the different sensors. In general, the different sensors compare as expected from their individual quantum efficiency. The R11265 is the only sensor with SBA cathode (35% peak quantum efficiency as compared to 25% for BA cathodes). It shows the highest photon yield with up to 29 detected photons per ring. Both the XP85012 MCPs and the Hamamatsu H8500 MAPMT show similar photon yields in the order of 21–22 hits/ring. During test beam operation, the H8500 MAPMTs showed the lowest dark count rate with only 10–20 Hz per channel (for a threshold of approx. 5% single photon peak). For the R11265 with SBA-cathode as well as the XP85012 MCP the dark rates were substantially higher, up to a few hundred Hz per channel.

3.3. Results based on ring fitting

The same algorithms for ring-fitting and -finding as developed for the full CBM RICH detector (see [7–9] for details) were also

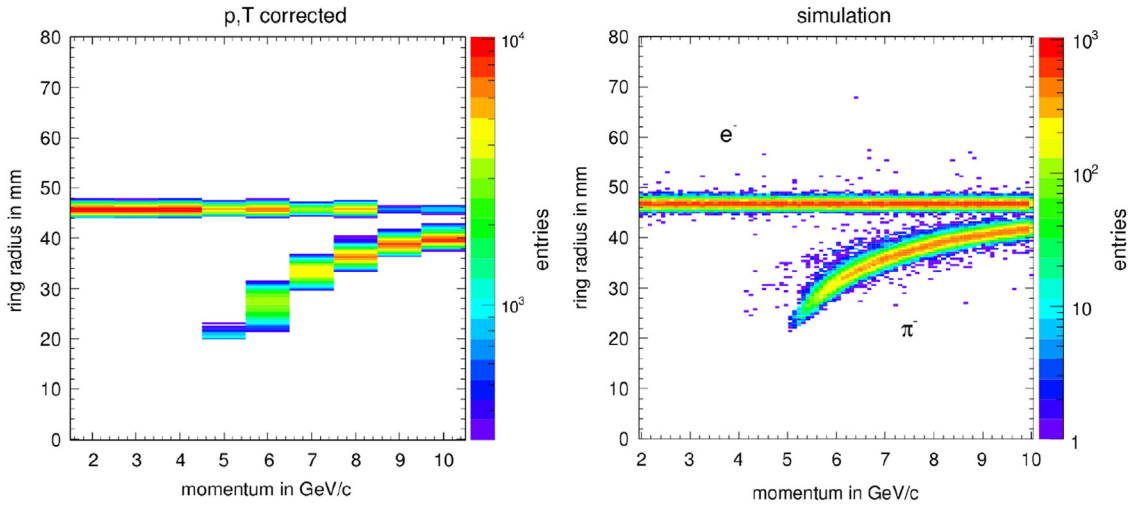

Fig. 8. Ring radius vs momentum for electron tracks in data (left) and simulation (right).

used for the prototype data. The fitted ring radius for electron rings is in the order of 46 mm, with a ring resolution after ring fitting in the order of 1.3%. The radius resolution is hardly worse for WLS-coated sensors, proving that chromatic dispersion of the radiator gas is only a minor contribution to the overall ring resolution. Also, isotropic fluorescence of WLS films does not significantly decrease the ring resolution. Ring radius as a function of momentum for electron and pion rings is shown in Fig. 8 for data (left), again in a very good agreement with the Monte Carlo simulation (right). The data were corrected for pressure and temperature which were permanently monitored during operation.

By implying a cut on the fitted ring radius around the electron radius (46 mm) particles passing the prototype detector were identified as electrons. Electron efficiency depends on the width of this cut, a trade between electron efficiency and pion suppression. The pion suppression factor (number of pions divided by number of pions misidentified as electrons) then could be extracted by comparing the external particle-ID information of the beamline Cherenkov counters. In Fig. 9 the achieved pion suppression factor as a function of particle momenta is shown for data and Monte Carlo, covering a range from 7 to 10 GeV/c (for electron efficiency of 95%). The data again are in a very good agreement with the simulations, a pion suppression by factor of 5000 is still reached at $p=8$ GeV/c. However, in the full RICH detector this number will be lower due to additionally required matching between particle tracks and Cherenkov rings, and due to the high track density. Nevertheless, it proves the reliability of the detector simulation.

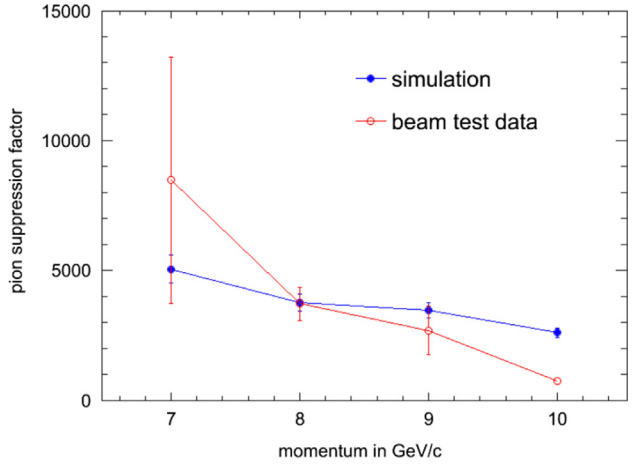

Fig. 9. Pion suppression factor for electron efficiency 95%.

4. R&D in the lab

The development of the CBM RICH is accompanied by a rich R&D program. This covers the evaluation of different mirror samples in terms of reflectivity, D0- and Ronchi test for mirror geometry, quantum efficiency measurements of various photon sensors, development of WLS coating techniques, and many more aspects. Here, we focus on a recent evaluation of photon sensor candidates by means of single photon efficiency scans. The first result for three different single sensors is shown in Fig. 10: The Hamamatsu H8500 (left side) is our baseline solution. Hamamatsu R11265 (middle) shows better single photon detection in terms of spectral shape and detection efficiency (it is available with SBA cathode). H12700 is a first prototype of a new tube combining the favorable dimensions and geometrical coverage of the H8500 with the single photon optimized dynode structure of the R11265. The upper line of scans compares the spatially resolved detection efficiency quantified as ≥ 1 hit detected per incident photon. The given efficiency index, calculated as relative efficiency averaged over the active area, allows for a direct comparison of the

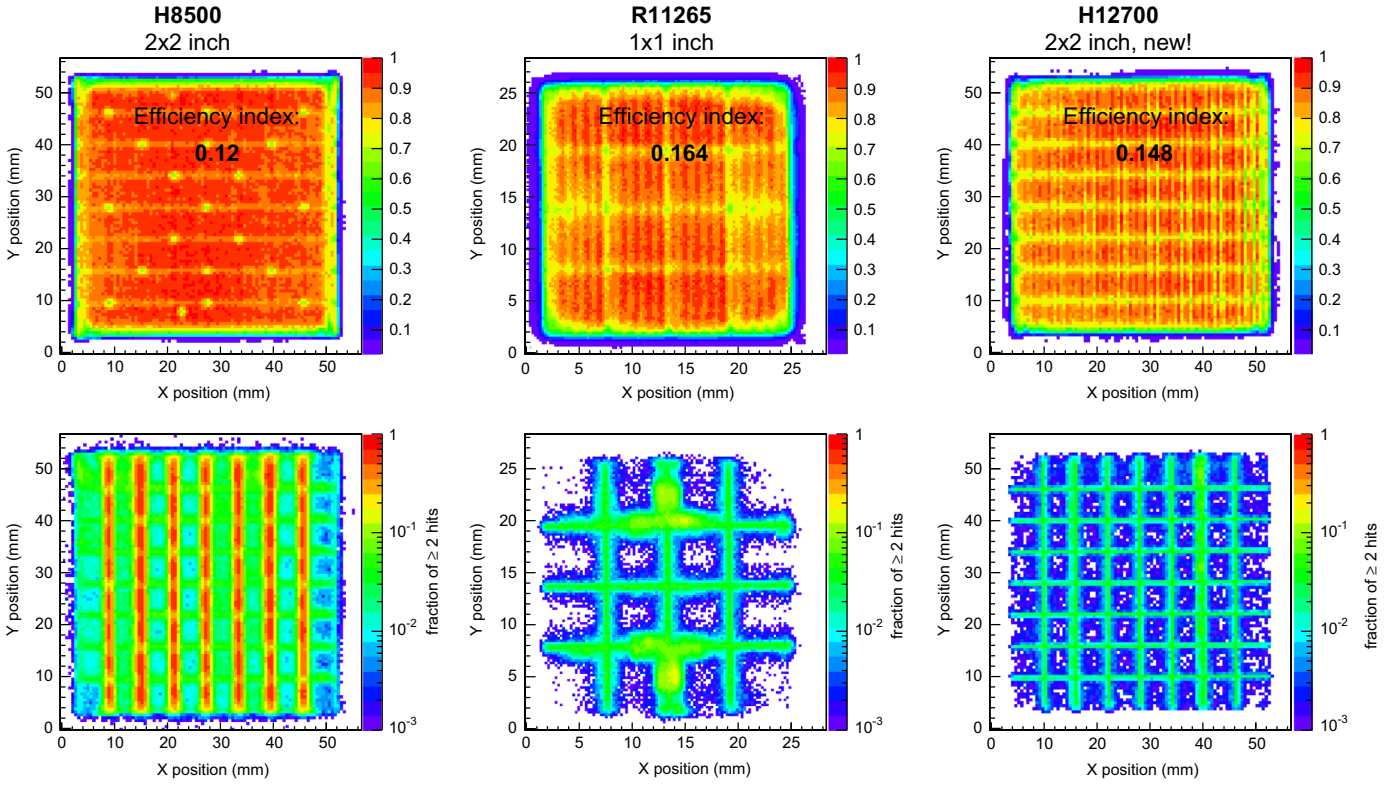

Fig. 10. Single photon *XY* -scans of Hamamatsu H8500 (left), R11265 (middle) and new H12700 (right). Upper line of scans: detection efficiency with ≥ 1 hit detected per incident photon; and lower line: cross talk as ≥ 2 hits detected.

overall detection efficiency. Interesting to note is the 20% higher efficiency index of the new H12700 compared to the H8500, despite both having only Bialkali cathodes. The nearly 35% higher efficiency of the R11265 is due to SBA cathode, but partly compensated by lower active area coverage. Pixel separation in case of the H8500 is worse, with increased cross talk/charge sharing (but also less dead space) between horizontally neighboring pixels. This becomes even more evident in the lower row of scans, based on events where ≥ 2 hits are being detected for a single incident photon. Here, the horizontal charge sharing in case of the H8500 is obvious. Both R11265 and the new H12700 show much better pixel separation (same logarithmic color scale for all three MAPMTs). According to our tests so far (based on a single H12700 prototype), the new H12700 seems to be a very promising alternative to the H8500 which is presently considered in several new RICH developments.

Acknowledgments

This work was supported by the Hessian LOEWE initiative through the Helmholtz International Center for FAIR, by the GSI F&E-Cooperation with Gießen and Wuppertal (WKAMPE1012), by BMBF Grants 05P12RGFCG, 05P12PXFCE and 05P09PXFC5, by the National Research Foundation of Korea (2012004024), by Helmholtz Grant IK-RU-002, and SC "ROSATOM" through FRRC.

References

[1] B. Friman, et al. (Eds.), The CBM Physics Book, Lecture Notes in Physics, vol. 814, Springer-Verlag, Berlin, Heidelberg 2011.
[2] J. Adamczewski-Musch, et al., Determination of tolerances of mirror displacement and radiator gas impurity for the CBM RICH detector, Nuclear Instruments and Methods in Physics Research Section A 766 (2014) 221.
[3] J. Adamczewski-Musch et al., Wavelength shifting films on Multianode PMTs with UV-extended window for the CBM RICH detector, this issue.
[4] CBM RICH collaboration, ⟨http://repository.gsi.de/record/65526⟩.
[5] C. Höhne, et al., Nuclear Instruments and Methods in Physics Research Section A 639 (2011) 294.
[6] A.S. Brogna, et al., Nuclear Instruments and Methods in Physics Research Section A 586 (2006) 301.
[7] J. Adamczewski-Musch, et al., Event reconstruction in the RICH detector of the CBM experiment at FAIR, Nuclear Instruments and Methods in Physics Research Section A 766 (2014) 250.
[8] S. Lebedev, et al., Journal of Physics: Conference Series 396 (2012) 022029.
[9] S. Lebedev, et al., in: PoS ACAT2010 060, 2010.